Available online at www.sciencedirect.com
ScienceDirect
Biosensors and Bioelectronics 23 (2007) 183–190
BIOSENSORS & BIOELECTRONICS
www.elsevier.com/locate/bios

# Integrated electrodes on a silicon based ion channel measurement platform

S.J. Wilk [a,*], L. Petrossian [a], M. Goryll [a], T.J. Thornton [a], S.M. Goodnick [a], J.M. Tang [b], R.S. Eisenberg [b]

[a] *Arizona State University, Center for Solid State Electronics Research, Tempe, AZ 85287, United States*
[b] *Rush Medical College, Department of Molecular Biophysics and Physiology, Chicago, IL 60612, United States*

Received 4 November 2006; received in revised form 12 March 2007; accepted 28 March 2007
Available online 8 April 2007

**Abstract**

We demonstrate the microfabrication of a low-noise silicon based device with integrated silver/silver chloride electrodes used for the measurement of single ion channel proteins. An aperture of 150 μm diameter was etched in a silicon substrate using a deep silicon reactive ion etcher and passivated with 30 nm of polytetrafluoroethylene via chemical vapor deposition. The average recorded noise in measurements of lipid bilayers was reduced by a factor of four through patterning of a 75 μm thick SU-8 layer around the aperture. Integrated electrodes were fabricated on both sides of the device and used for repeatable, stable, giga-seal bilayer formations as well as characteristic measurements of the transmembrane protein OmpF porin.


*Keywords:* Ion channels; Lipid bilayers; Microfabrication

## 1. Introduction

The detection and transduction of signals from specific, single molecules is the main key to biological sensors. Sensors that can more accurately respond to lower concentrations of target analytes increase the detection capabilities of a given system. One of nature's sensors is the transmembrane ion channel protein, which directly responds to both single molecules and physical stimuli (Bayley and Cremer, 2001). These proteins form pores through the highly resistive cell membrane and allow for diffusion of ions and small molecules from one side to the other. One of the unique features of ion channel proteins is that they show gating mechanisms superficially similar to transistors when a bias is applied to the gate (Sigworth and Klemic, 2002). In the case of voltage gated proteins, a potential applied across the membrane results in a change of the conductance of the channels imbedded within. Ligand gated channels exhibit similar conductance changes when a binding event occurs. Another unique feature of ion channel proteins is that some are very specific towards which ionic species pass through their pore. For example, voltage gated potassium channels allow $K^+$ ions to permeate at least 10,000 times more easily than $Na^+$ (Doyle et al., 1998). The combination of signal transduction via gating mechanisms and high selectivity towards specific molecules makes ion channel proteins a highly desirable candidate for a biological sensor.

Recently, it has been shown that α-hemolysin, a non-specific bacterial toxin channel protein, can be genetically engineered modifying the inner pore regions so specific analytes can be detected and identified (Bayley and Cremer, 2001; Bayley and Jayasinghe, 2004; McGeoch et al., 2000). This technique results in two types of information about the analyte molecule. First is the actual magnitude of the conductance change due to the particular molecule bound in the pore and is measured as a change in the current flowing through the protein. The second is the amount of time the molecule spends bound inside the pore. This information provides stochastic signatures of particular analytes using the same protein. The incorporation of engineered proteins into ion channel measurement platforms will result in a highly selective sensor capable of providing stochastic information of particular analytes of interest.

Ion channel measurements have traditionally been conducted using the patch-clamp technique first reported by Neher and Sakmann (1976). The technique was further improved upon in

* Corresponding author.
*E-mail address:* seth.wilk@asu.edu (S.J. Wilk).

0956-5663/$ – see front matter © 2007 Elsevier B.V. All rights reserved.
doi:10.1016/j.bios.2007.03.030

the early 1980's with the introduction of the giga-seal, a high resistance seal between a cell membrane and a patch recording pipette tip (Hamill et al., 1981; Sigworth and Neher, 1980). A giga-seal forms when a piece of a cell membrane is suctioned into a suitable pipette tip, which results in a very high resistance seal measured in giga-ohms. This seal corresponds to a very low leakage path between the membrane and pipette tip for ions in the surrounding electrolyte solution and is crucial for the accurate measurement of single ion channel currents.

Another method for forming lipid bilayer membranes with monolayers of lipids on the surface of a solution was introduced in 1972 (Montal and Mueller, 1972; White, 1986). Two baths, connected with a central small diameter hole in a sheet of Teflon, were lowered and then raised over the aperture. A monolayer of lipid, present on the surface of the solution, comes together during this raising and lowering process and forms a bilayer separating the two baths (Montal and Mueller, 1972). This work stemmed from the physical painting of a bilayer using lipid dissolved in large amounts of organic solvent across a small aperture originally performed by Mueller et al. (1962, 1963). These techniques allowing for the formation of a lipid bilayer membrane in vitro across a small aperture are referred to in the literature collectively as Montal–Mueller methods, and are a main step in the process known as ion channel reconstitution. Ion channel reconstitution removes an ion channel protein out of a native cell membrane and by incorporating it into a bilayer formed utilizing the above techniques, allows for a measurement of the channel in a simpler, well defined environment. The ion channels are inserted into the bilayer using either vesicle fusion techniques (Cohen et al., 1980; Hanke, 1986; Schindler and Rosenbusch, 1978) or protein self-insertion (van der Straaten et al., 2003; Wilk et al., 2004). The common material used for these methods is Teflon, or another suitably hydrophobic material, which allows for favorable interactions between the lipids and substrate. The lipid membranes span openings in the Teflon sheet that are typically ~100 μm in diameter and formed by electrical spark discharges or mechanical drilling. Neither method lends itself to reproducible pore formation or to the batch manufacturing that would be required for large volume production of ion channel based biosensors. In contrast, CMOS microfabrication technologies are very well suited to the large scale production of silicon based pores with precisely controlled geometries. In this work, we demonstrate that 150 μm diameter pores can be routinely fabricated in silicon substrates. After coating the surface with a hydrophobic PTFE layer Montal–Mueller methods can be used to span lipid bilayers across the silicon apertures and form high resistance giga-seals.

Efforts have been made to measure ion channel proteins using microfabricated devices which target both patch-clamp and reconstitution measurements. Researchers have focused on fabricating small apertures in glass (Fertig et al., 2002), $Si/SiO_2$ (Goryll et al., 2004; Matthews and Judy, 2006; Pantoja et al., 2004; Wilk et al., 2004, 2005a,b) and polymer materials (Klemic et al., 2002; Malmstadt et al., 2006; Mayer et al., 2003). Different issues such as ease of fabrication, noise properties of the final device and the ability to form a high resistance giga-seal, suitable for single channel measurements, have been addressed. The formation of a giga-seal between the lipid bilayer and substrate is critical for single channel measurement because it determines the leakage current of the system. High leakage current will wash out signals resulting from ion channels with low conductances.

Here, we focus on a microfabricated silicon system which targets ion channels inserted into lipid bilayers formed with Montal–Mueller reconstitution techniques. Silicon provides an ideal substrate because arrays of devices can be precisely manufactured and finally integrated with both microfluidics and microelectronics. We have previously demonstrated a polytetrafluoroethylene (PTFE, Teflon) coated silicon device suitable for reproducibly forming high resistance seals between a lipid bilayer and substrate (Wilk et al., 2004). We have enhanced the capabilities of the device by first patterning an SU-8 layer onto the surface to reduce the noise and then integrating silver/silver chloride electrodes around the aperture. The electrodes allowed for stable measurements of single channels of OmpF porin proteins which were self-inserted into lipid bilayers formed on the device. This device demonstrates significant advances towards completely integrating and measuring the formation of artificial lipid bilayers and inserted proteins of interest utilizing silicon technology. Incorporation of engineered proteins such as α-hemolysin into a fully integrated reconstitution platform will provide functional biosensors with single molecule detection capabilities.

## 2. Materials and methods

### 2.1. Device fabrication

Samples were prepared using 4 in. diameter, double-sided polished Si (1 0 0) wafers having a thickness of 440 μm. The substrates were patterned using photolithography and standard AZ4330 resist spun to a final thickness of 4.1 μm. The resist was patterned on a Canon 501FE mask aligner and developed in AZ300MIF supplied by AZ Chemicals. The silicon etches were completed in a deep silicon reactive ion etcher (STS Advanced Silicon Etcher) using the Bosch process. The Bosch process is a cyclic etch which first passivates using $C_4F_8$ as the source gas and then etches using $SF_6$ and $O_2$ as the source gases to provide for vertical sidewalls (Ayón et al., 1999). The first process step was to thin a 1 mm diameter region of the wafer to a final thickness of 150 μm using the STS deep silicon etcher (Fig. 1(A)). The thinning etch was optimized to allow for high etch rates and selectivity with a concave bottom with gas flow rates of 90 sccm of $C_4F_8$ for 7 s to passivate and then 136 sccm of $SF_6$ for 14.8 s with 0.7 s overlap for the etch step. Next, backside lithography using an EV Group 620 aligner was used to define an aperture in the center of the thinned region which was also etched in the STS deep silicon etcher (Fig. 1(B)). The aperture was designed to have a 150 μm diameter similar to that currently used for Teflon and commercial devices. The microfabricated aperture and thinned region have an aspect ratio of 1:1 (diameter to height of the aperture) which is desirable for planar lipid bilayer formation. The aperture etch recipe was optimized for an aspect ratio independent etch rate. Gas flow rates were 85 sccm of $C_4F_8$ for 6 s to passivate and then 130 sccm of $SF_6$ and 13 sccm of $O_2$

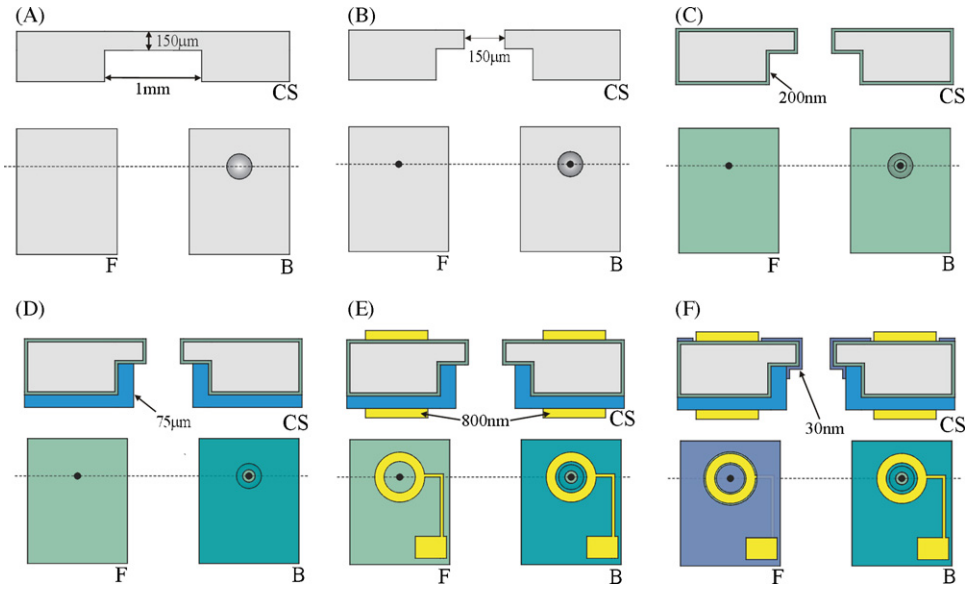


Fig. 1. Cross-section and top views of the integrated silicon device for transmembrane ion channel measurements after each step of fabrication where CS stands for cross sectional view, F stands for frontside view and B stands for backside view. (A) A 1 mm recess is etched into the backside of a silicon substrate. (B) Using backside alignment techniques and a deep silicon etch process, a 150 μm diameter aperture is etched through the center of the recessed region. (C) The surface is thermally oxidized with 300 nm of silicon dioxide. (D) A noise reducing 75 μm thick SU-8 layer is patterned on the backside of the device. (E) Silver is evaporated and wet etched to form electrodes on both sides of the device. (F) PTFE is chemically vapor deposited on the surface of the device using lift-off techniques to remove the material from over the active area of integrated electrodes.

for 12 s to etch. After etching the aperture, a thermal oxidation of 200 nm followed to produce an electrically insulating layer on the surface (Fig. 1(C)). The device was then coated with 75 μm of SU-8 and patterned using conventional photolithography, so that resist entered the thinned region thus decreasing the overall capacitance of the device (Fig. 1(D)). Next, 8000 Å of silver was evaporated onto the surface of both sides of the wafer with a CHA 600-SE electron beam evaporator. AZ4330 resist was patterned on top of the silver layer and then etched with a 1:1:20 mixture of sodium hydroxide, hydrogen peroxide and water (Fig. 1(E)). On the side of the device with exposed oxide, a 20 nm adhesion layer of titanium was deposited prior to silver deposition. A 30 nm PTFE layer was then chemically vapor deposited using the deep reactive ion etcher and $C_4F_8$ as the gas source (Fig. 1(F)). In order to keep the PTFE from coating the electrodes and insulating them from electrolyte solution, 1 μm of OCG825 was first patterned over the electrodes and used to lift-off the deposited PTFE. Finally, the electrodes were chloridized in 5% NaOCl before experimental measurements were taken. All fabrication was performed at Arizona State University in the Center for Solid State Electronics Research cleanroom.

### 2.2. Lipid bilayer characteristics

Lipid bilayer experiments were performed using a Teflon bilayer chamber with a 5 mm diameter opening between two baths of electrolyte solution. Both baths were filled with 3 ml KCl solution (1.0 M for the bilayer measurements and 0.5 M for the OmpF porin measurements), buffered with 20 mM *N*-(2-hydroxyethyl) piperazine-*N*′-(2-ethanesulfonic acid) (HEPES) at pH 7.4. The silicon device was sandwiched between the baths with the aperture in the center of the opening. Lipids (1,2-dioleoyl-sn-glycero-3-phosphoethanolamine and 1,2-dioleoyl-sn-glycero-3-phosphocholine) (DOPE:DOPC, 4:1) were dissolved in *n*-decane (10 mg/ml) and used to form a bilayer with the techniques of Montal and Mueller (Montal and Mueller, 1972; Mueller et al., 1962; Mueller et al., 1963). Current and bilayer capacitance were measured using an Axon Instruments Axopatch 200B current amplifier and a National Instruments DAQ PCI card programmed with LabVIEW software. Recordings using the Axopatch were performed at a sampling rate of 5 kHz and filtered with a four-pole low-pass Bessel filter with cutoff frequency of 2 kHz. In order to test for true bilayer membranes, several different methods including monitoring the system's impedance and applying short voltage pulses (Vpulse >1.2 V) were used. The bilayer resistance was derived from the slope of the current–voltage (*I–V*) response due to a 1 s duration ramping potential from negative to positive. Capacitance was calculated using the RC time constant of the current response due to a square wave applied prior to the *I–V* sweep. Bilayer resistances of 1–20 GΩ, total system capacitance of >30 pF and immediate rupture due to the applied voltage pulses indicated bilayers suitable for inserting ion channel proteins. Thick 'membranes' of lipid routinely showed resistances >20 GΩ, total system capacitances <30 pF and could not be ruptured by the voltage pulse which we attributed to unstructured volumes of phospholipid and organic solvent blocking the aperture. The bilayer was then reformed and measured for correct impedance after rupturing. Finally, ion channels were self-inserted into the membrane by adding OmpF porin to the trans (ground side) bath.

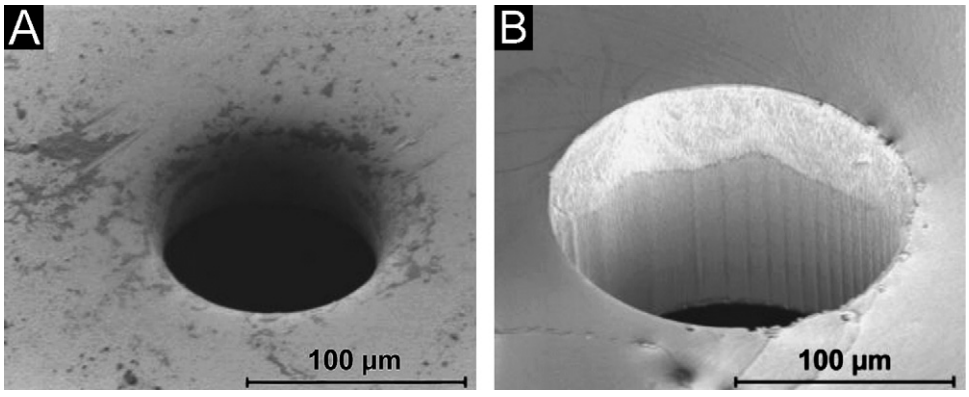


Fig. 2. (A) Tilted plan-view SEM image of an aperture in a 25 μm thick Teflon sheet created by electrostatic discharge. Due to the nature of the hole formation process the sidewall is completely rounded and smooth. (B) SEM image of an aperture formed in silicon using deep reactive ion etching. The sidewalls are vertical, exhibiting the roughness induced by the cyclic etch and deposition process. The small notches close to the edge of the aperture are due to plasma punch-through effects before the material in the center is removed.

## 3. Results and discussion

### 3.1. Device characteristics

The main goal of this research was to demonstrate that silicon could be used as a substrate for low noise measurements of suspended bilayers and transmembrane ion channel proteins. The devices were fabricated with 150 μm diameter apertures with a sidewall length of 150 μm resulting in an aspect ratio of 1:1. This aspect ratio is important because it increases both the probability of true bilayer formation and stability of the membrane. In order to achieve this ratio, the devices were fabricated in a two etch step process using the Bosch process and backside alignment. A thermal oxide of 200 nm was then used to electrically isolate the silicon substrate from electrolyte solution. These devices were initially used to form lipid bilayers but it was found that the formation was very difficult which we attributed to the hydrophilic oxide layer. In order to make bilayer formation more probable, the surface was made hydrophobic with a chemical vapor deposition of PTFE after electrode fabrication as described below.

Fig. 2 allows for a comparison of the shape and microstructure of the aperture created using reactive ion etching (B) and an aperture created by electric discharge across a 25 um thick Teflon sheet (A). Although the diameter is similar (the hole formed by electric discharge is 100 um wide, while the hole in the silicon substrate is 150 um wide), the shape of the apertures is significantly different. The hole in the Teflon sheet shown in Fig. 2A exhibits smooth edges and does not show a vertical sidewall profile. On the other hand, the aperture etched in silicon (Fig. 2B) has perfectly straight sidewalls, sharp edges and a slight surface roughness caused by the cyclic Bosch etching process. Despite the differences in shape, after surface passivation with PTFE reproducible high resistance bilayers were easily formed on the silicon based device (Table 1).

One of the main components in ion channel measurements is the electrodes which act as a transducer of ionic current into electric current. Silver/silver chloride (Ag/AgCl) wire electrodes are commonly used by many electrophysiologists because they have a low resistance, do not polarize when constructed properly and have a relatively low temperature coefficient (Fry and Langley, 2001). Silicon microfabrication techniques allow for

Table 1
Lipid bilayer seal resistance and calculated RMS current noise for microfabricated devices

| Device with only PTFE layer | | Device with SU-8 and PTFE layers | | Integrated electrode device | |
|---|---|---|---|---|---|
| Resistance (GΩ) | RMS noise (pA) | Resistance (GΩ) | RMS noise (pA) | Resistance (GΩ) | RMS noise (pA) |
| 8.5 | 6.28 | 9.7 | 1.48 | 5.00 | 1.45 |
| 11.3 | 5.98 | 13.2 | 1.38 | 5.00 | 1.15 |
| 12.2 | 5.73 | 7.1 | 1.50 | 4.80 | 1.24 |
| 13.3 | 5.64 | 12.7 | 1.49 | 6.30 | 1.05 |
| 14.2 | 5.62 | 18.4 | 1.49 | 20.20 | 1.27 |
| 16.7 | 5.05 | 18.9 | 1.43 | 25.10 | 1.49 |
| Averages | | | | | |
| 12.70 | 5.72 | 13.33 | 1.46 | 11.07 | 1.28 |
| Relative standard deviation | | | | | |
| 21.84% | 7.20% | 35.04% | 3.22% | 82.42% | 13.33% |

Table showing representative resistances and calculated noise for bilayers formed on a silicon device with a PTFE coating, the same device with noise reducing SU-8 layer and a fully integrated device with Ag/AgCl electrodes microfabricated on the surface. The bottom rows show the averages and relative standard deviation of each column.

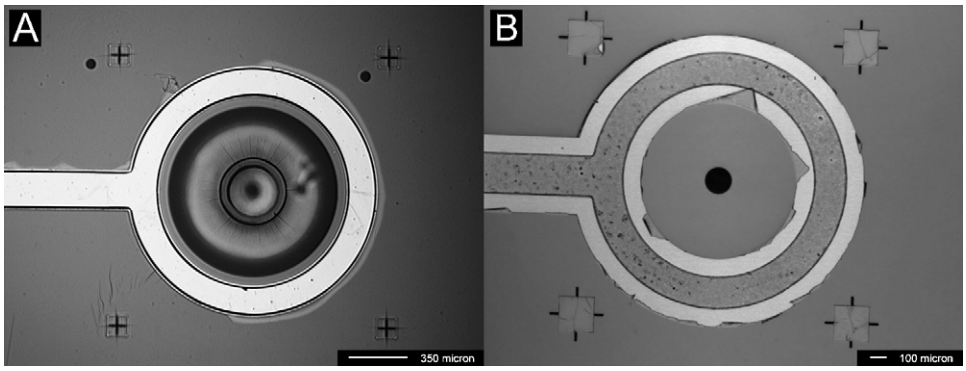


Fig. 3. (A) Micrograph of the silicon integrated device from the backside with an additional 10 μm thick layer of SU-8 2010 patterned 15 μm over the edge of the Ag/AgCl electrodes. This additional layer helps to keep the electrodes attached to the surface of the SU-8 during measurements in electrolyte solution. (B) Micrograph viewed from the front-side of the device showing the lifted-off PTFE layer around the silver electrode. The 150 μm aperture in the middle is completely coated with a 30 nm PTFE layer.

evaporation and subsequent deposition of metals and other materials and provide an attractive means for fabricating electrodes near an aperture used for ion channel protein measurements. In an effort to reduce electrode vibration, increase surface area and position the electrodes as close to the aperture as possible, Ag/AgCl electrodes were microfabricated directly on the surface of our device a radial distance of 565 μm from the center of the aperture. Silver was evaporated using an electron beam evaporator to a final thickness of 800 nm. Initially, thinner electrodes of 200 nm thickness were fabricated but they tended to peel off the silicon substrate after chloridization during immersion and measurement in electrolyte solution. Electrodes on the SU-8 coated side tended to peal off even after increasing their thickness, so an additional SU-8 2005 5 μm hold down layer was patterned over its outer edges (Fig. 3A). The final thicker 800 nm electrodes were tested for stability and long-term usability both by measuring the Nernst potential developed between them due to different KCl concentrations in each bath as well as by applying a known potential and measuring the resultant current (Goryll et al., 2004). Using these methods, the electrodes were demonstrated to maintain a stable reference voltage as well as pass sufficient currents that are several orders of magnitude higher than those expected during actual ion channel measurement.

In order to passivate the silicon surface, the devices were then coated with a 30 nm PTFE layer to lower the surface energy and render the surface hydrophobic. Previously we demonstrated that this PTFE layer greatly increased the seal resistance between a lipid bilayer and silicon substrate which allowed for the repetitive formation of giga-seal resistances (Wilk et al., 2004). The PTFE layer was deposited on the topside of the device after electrode fabrication and therefore had to be patterned around the Ag/AgCl electrode so the layer did not insulate the electrode from the electrolyte bath solutions. The PTFE was lifted off over the electrode area by first patterning OCG825 positive photoresist and subsequently chemically vapor depositing the PTFE layer and immersing it in acetone for 5 min. Fig. 3B shows the device after passivation where the small triangular remainders in the lift-off region are sections of PTFE that are not attached to the substrate except at the edges of the region. Plasma deposited PTFE is characterized as an amorphous network of branching polymer (Washo, 1976). These patches demonstrate that the PTFE layer forms a stable film with strong adhesion to the oxide layer because the PTFE remainders are only mechanically attached at the edges.

### 3.2. Lipid bilayer formation

After device fabrication, lipid bilayers were formed using painting techniques such that a small amount of lipid in decane solvent was brushed across the microfabricated aperture. Following bilayer formation, a voltage ramp was applied across the membrane and the slope of the resultant current–voltage (*I–V*) trace was used to determine the resistance of the membrane. The resistance of bilayers formed on the different devices was repeatedly in the giga-ohm range and are adequate for ion channel measurement. Bilayers showing desirable measured impedances and the ability to be ruptured with a voltage pulse were easily formed on the PTFE coated devices within several minutes. However, the first attempt was often experimentally determined to be a thick unstructured lipid-decane volume which was then physically removed. Subsequent attempts led to the formation of lipid bilayers suitable for ion channel insertion that would routinely last for several hours suspended across the devices. Several lipid bilayers on PTFE coated devices lasted for over 5 h which was much longer than necessary for OmpF measurements (Wilk et al., 2005b). The estimated capacitance of the bilayer contribution to overall system capacitance is $60 \pm 20$ pF, which results in a specific capacitance of $\sim$0.4 μF/cm$^2$ based on the area of the aperture. The specific capacitance of cell membranes is normally on the order of 1 μF/cm$^2$ (Hille, 2001). Our results have lower specific capacitance because the outer annulus of the bilayer in the aperture is comprised of a radially bisected torus region containing a thick rim of lipid and decane solvent. Future experiments such as impedance spectroscopy measurements will correlate the exact surface area of the bilayer only region with the measured capacitance. The current noise was calculated by subtracting the slope from the measured *I–V* data

and then computing the RMS noise. Seal resistance and corresponding current noise is shown for a sample of high resistance bilayers formed on different devices in Table 1. The data selected for noise analysis is representative of an average data set of each of the systems and was not the lowest noise achieved.

### 3.3. Noise characteristics

A major issue in ion channel measurements is the overall background noise level due to the platform used in experimentation. Many different methods have been used to lower the noise of patch-clamp pipette tips including coating with PDMS (Levis and Rae, 1992). An advantage of microfabrication is that different layers can be integrated onto a device with very precise control of dimensions. Here, a 75 μm thick SU-8 layer has been patterned onto the backside thinned region before electrode fabrication and device passivation with a final inner diameter of 250 μm.

A comparison of lipid bilayers formed on a silicon device without, and another with, the micropatterned SU-8 layer show average RMS current noises of 5.72 pA and 1.46 pA, respectively (Table 1). This change corresponds to the reduction in capacitance of the device from 1 nF to 80 pF and follows the dielectric noise contribution ($i_d$) to overall measured noise described in units of the root mean square of ampere squared ($A^2$ RMS) as (Levis and Rae, 1992; Mayer et al., 2003; Sherman-Gold, 1993; Wonderlin et al., 1990):

$$i_d = \sqrt{4kTDC_t B^2} \qquad (A^2\,\text{RMS})$$

where $k$ is Boltzmann's constant, $T$ the temperature, $D$ the thermal dissipation factor found in look-up tables for different materials, $C_t$ is the total capacitance (the sum of both membrane and device capacitance) and $B$ is the bandwidth. During measurement, a circular region of 5 mm diameter of the device was exposed to the bath solutions which simplified access for bilayer formation but resulted in overall higher capacitance.

For devices coated with SU-8, a slight reduction in the average of measured noise between the external wire electrodes (1.46 pA) and the integrated electrodes (1.28 pA) was also recorded which we attribute to slight process variations and external noise in the measurement. A lipid bilayer was formed on the fully integrated device and first measured with external wire electrodes which were then switched while maintaining continuity to the integrated electrodes. This resulted in an almost identical RMS noise of 1.22 pA and 1.15 pA for the same bilayer measured with external and integrated electrodes respectively (Fig. 4A and B). This measurement shows that the integrated electrodes much nearer the aperture than the external Ag/AgCl wire electrodes do not reduce the noise of the measurement significantly. Fig. 4C also shows an $I$–$V$ trace of a lipid bilayer formed on a different device without the SU-8 layer for comparison purposes. One prominent feature in Fig. 4C is that because the voltage sweep protocol used first applied a negative bias of −100 mV, an asymmetry in measured current due to capacitive charging was recorded.

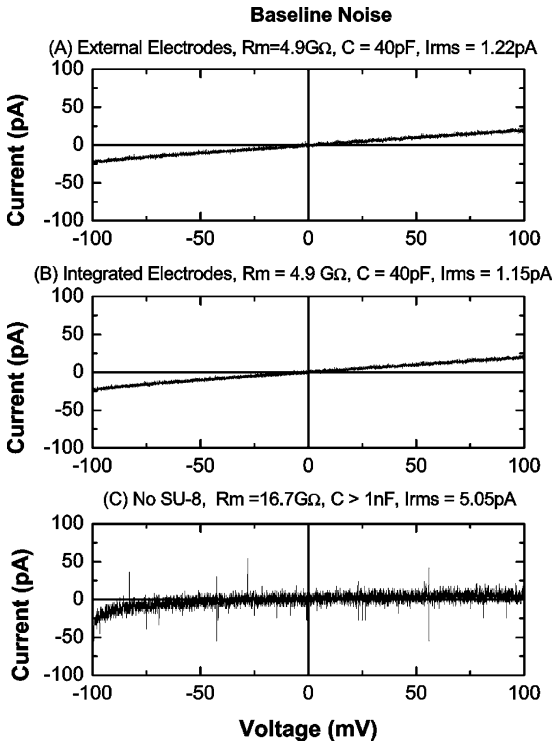


Fig. 4. Current–voltage sweeps used to calculate seal resistance and RMS current noise of bilayers formed on the microfabricated silicon device. The same bilayer was measured with two different sets of electrodes on one device. (A) A lipid bilayer formed on the integrated device with the SU-8 layer and microfabricated Ag/AgCl electrodes but measured with external wire electrodes. (B) The same bilayer measured in (A) but with the electrodes switched to the integrated electrodes without rupturing the bilayer. (C) A lipid bilayer of similar composition to A and B formed on a different PTFE coated silicon device without the SU-8 layer, measured with external electrodes, shows an RMS noise level four times higher than those with the layer.

### 3.4. OmpF porin measurements

After formation of a stable lipid bilayer, OmpF porin ion channel protein was added to the trans bath and then self-inserted into the membrane after several minutes of stirring. OmpF porin is a trimer with three individual channels per protein that open or close due to an applied potential across the membrane. As the potential increases, the channels are more likely to close and reduce the total current through the system with characteristic conductance steps. The conductance of the channels is also determined by the electrolyte concentration and pH of the solution used for experimentation (van der Straaten et al., 2003). One method employed to determine protein insertion and conductance levels was a current voltage sweep of the system, similar to those used for bilayer seal resistance calculations above. Initially, a small $I$–$V$ slope is recorded indicating a high resistance bilayer. Upon insertion of ion channel proteins, the slope rapidly increases in discrete levels where each step correlates to the conductance of a single channel. Fig. 5 shows the insertion and measurement of OmpF porin using the microfabricated Ag/AgCl electrodes where trace one shows the initial high resistance bilayer and actual insertion event of a single protein with two open channels. Measurements were made of the same

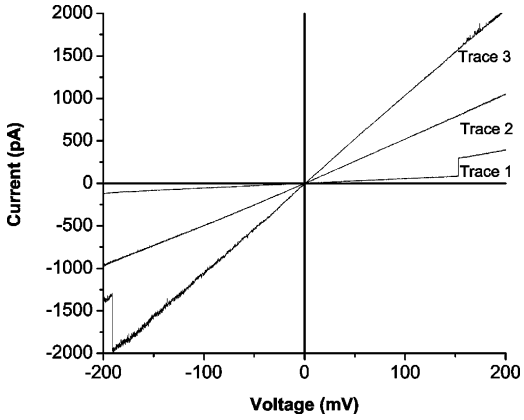


Fig. 5. Measurement of the insertion of OmpF porin using the microfabricated integrated electrodes on the surface of the silicon device in 0.50 M KCl solution. Trace one shows the baseline resistance with the insertion of an OmpF porin protein and the open state of two channels. Trace two shows the measurement of two complete proteins (6 open channels, $t = 19$ s) while trace three shows the measurement of additional open channels (13 total open channels, $t = 172$ s). The time with reference to the first baseline plot shows typical rates of porin insertion. The number of channels was determined using a single channel conductance of 0.7 nS which is typical for OmpF porin in 0.5 M KCl.

system over time and show 2 open channels (trace 2, $t = 19$ s) and 13 open channels (trace 3, $t = 172$ s). The number of channels was determined based on a single channel conductance of 0.7 nS which is commonly reported for OmpF porin in 0.5 M KCl (Schindler and Rosenbusch, 1978; Schirmer, 1998; van der Straaten et al., 2003). In addition, OmpF porin was also measured using a Warner bilayer cup on the same measurement set up as the silicon devices and was shown to have a similar single channel conductance.

Measurements were also made of the switching nature of OmpF porin due to an applied potential. Nonspecific porin channels have been demonstrated to exhibit voltage-gating in response to larger (~100–200 mV) transmembrane potentials (Nikaido, 2003; Schindler and Rosenbusch, 1978). The type

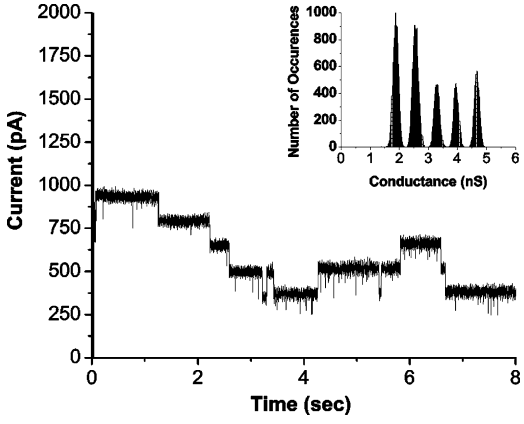


Fig. 6. Single channels of OmpF porin in 0.50 M KCl, 20 mM HEPES, at pH 7.4 measured using the integrated electrodes on the PTFE coated, SU-8 patterned, silicon device at a holding potential of 200 mV. The difference between peaks indicates a conductance of 0.7 nS per channel which is consistent with results found in the literature.

of gating exhibited by porins is described as two-state gating with closing of the pore at both positive and negative potentials (Bainbridge et al., 1998). Fig. 6 shows the measured gating of OmpF porin as a function of time with a potential of 200 mV held across the membrane using the microfabricated integrated electrodes. The inset of Fig. 6 shows a histogram of the conductance calculated from the time plot with individual peaks spaced 0.7 nS apart which is the same conductance reported by others in the literature (Schindler and Rosenbusch, 1978; Schirmer, 1998; van der Straaten et al., 2003).

## 4. Conclusions

We have demonstrated the microfabrication of an integrated silicon based device with Ag/AgCl electrodes used to measure conductance fluctuations of single ion channel proteins. The Bosch process was used to etch an aperture of 150 μm diameter in a silicon substrate with a 1:1 aspect ratio suitable for bilayer membrane formation. A 75 μm thick SU-8 layer was patterned around the aperture which reduced the capacitance of the device and the resulting dielectric noise so that the measured RMS current noise of lipid bilayers was reduced by a factor of four. Stable Ag/AgCl integrated electrodes were fabricated using an electron beam evaporator to deposit silver which was subsequently immersed in household bleach for chloridization. These electrodes demonstrated desirable characteristics for lipid bilayer and single ion channel measurement although they did not definitively reduce the noise of the system. PTFE was then chemically vapor deposited on the surface to help ensure a high resistance seal with a lipid bilayer. Repeatable formations of a lipid bilayer across the aperture were achieved and seal resistances in the GΩ range were measured. Characteristic measurements of OmpF porin channels were made on the silicon device using the integrated electrodes and found to be similar to those previously measured.

Microfabrication of the aperture offers the advantage of precise control of the diameter and high volume throughput over the common method of drilling or burning a hole in a thin sheet of Teflon. Using these techniques, large arrays can be easily manufactured for different sensing applications. Here, the final device is completely integrated with Ag/AgCl electrodes and exhibits low-noise performance levels suitable for measurements of transmembrane ion channel proteins. The incorporation of engineered proteins into this platform will result in a highly selective sensor capable of providing stochastic information of particular analytes of interest. Further integration of microfluidics to deliver both phospholipids for fluidic bilayer painting as well as target analyte molecules will result in a fully integrated biosensor capable of single molecule recognition.

## Acknowledgements

This work was supported by the Defense Advanced Research Projects Agency as part of the MOLDICE program. Student support in part was from the National Science Foundation IGERT program.

## References


Ayón, A.A., Braff, R., Lin, C.C., Sawin, H.H., Schmidt, M.A., 1999. J. Electrochem. Soc. 146 (1), 339–349.

Bainbridge, G., Gokce, I., Lakey, J.H., 1998. FEBS Lett. 431 (3), 305–308.

Bayley, H., Cremer, P.S., 2001. Nature 413 (6852), 226–230.

Bayley, H., Jayasinghe, L., 2004. Mol. Membr. Biol. 21 (4), 209–220.

Cohen, F.S., Zimmerberg, J., Finkelstein, A., 1980. J. Gen. Physiol. 75 (3), 251–270.

Doyle, D.A., Cabral, J.M., Pfuetzner, R.A., Kuo, A.L., Gulbis, J.M., Cohen, S.L., Chait, B.T., MacKinnon, R., 1998. Science 280 (5360), 69–77.

Fertig, N., Blick, R.H., Behrends, J.C., 2002. Biophys. J. 82, 3056–3062.

Fry, C.H., Langley, S.E.M., 2001. Ion-Selective Electrodes for Biological Systems. Harwood Academic Publishers.

Goryll, M., Wilk, S., Laws, G.M., Thornton, T., Goodnick, S., Saraniti, M., Tang, J., Eisenberg, R.S., 2004. 4th IEEE Conference on Nanotechnology, Munich, Germany, pp. 302–304.

Hamill, O.P., Marty, A., Neher, E., Sakmann, B., Sigworth, F.J., 1981. Pflugers Archiv-Eur. J. Physiol. 391 (2), 85–100.

Hanke, W., 1986. In: Miller, C. (Ed.), Ion Channel Reconstitution. Plenum Press, New York, pp. 141–153.

Hille, B., 2001. Ion Channels of Excitable Membranes, Third Edition. Sinauer Associates, Inc.

Klemic, K.G., Klemic, J.F., Reed, M.A., Sigworth, F.J., 2002. Biosens. Bioelectron. 17 (6–7), 597–604.

Levis, R.A., Rae, J.L., 1992. Methods Enzymol. 207, 14–66.

Malmstadt, N., Nash, M.A., Purnell, R.F., Schmidt, J.J., 2006. Nano Lett. 6 (9), 1961–1965.

Matthews, B., Judy, J., 2006. J. Microelectromech. Syst. 15 (1), 214–222.

Mayer, M., Kriebel, J.K., Tosteson, M.T., Whitesides, G.M., 2003. Biophys. J. 85, 2684–2695.

McGeoch, J.E.M., McGeoch, M.W., Carter, D.J.D., Shuman, R.F., Guidotti, G., 2000. Med. Biol. Eng. Comput. 38, 113–119.

Montal, M., Mueller, P., 1972. Proc. Natl. Acad. Sci. U. S. A. 69 (12), 3561–3566.

Mueller, P., Tien, H.T., Wescott, W.C., Rudin, D.O., 1962. Circulation 26 (5), 1167–1171.

Mueller, P., Wescott, W.C., Rudin, D.O., Tien, H.T., 1963. J. Phys. Chem. 67 (2), 534–535.

Neher, E., Sakmann, B., 1976. Nature 260 (5554), 799–802.

Nikaido, H., 2003. Microbiol. Mol. Biol. Rev. 67 (4), 593.

Pantoja, R., Nagarah, J.M., Starace, D.M., Melosh, N.A., Blunck, R., Bezanilla, F., Heath, J.R., 2004. Biosens. Bioelectron. 20 (3), 509–517.

Schindler, H., Rosenbusch, J.P., 1978. Proc. Natl. Acad. Sci. U. S. A. 75 (8), 3751–3755.

Schirmer, T., 1998. J. Struct. Biol. 121 (2), 101–109.

Sherman-Gold, R., 1993. The Axon Guide for Electrophysiology and Biophysics: Laboratory Techniques. Axon Instruments, Foster City, CA.

Sigworth, F.J., Klemic, K.G., 2002. Biophys. J. 82, 2831–2832.

Sigworth, F.J., Neher, E., 1980. Nature 287 (5781), 447–449.

van der Straaten, T.A., Tang, J.M., Ravaioli, U., Eisenberg, R.S., Aluru, N.R., 2003. J. Comput. Electron. 2 (1), 29–47.

Washo, B.D., 1976. J. Macromol. Sci.-Chem. A 10 (3), 559–566.

White, S.H., 1986. In: Miller, C. (Ed.), Ion Channel Reconstitution. Plenum Press, New York, pp. 3–32.

Wilk, S.J., Goryll, M., Laws, G.M., Goodnick, S.M., Thornton, T.J., Saraniti, M., Tang, J., Eisenberg, R.S., 2004. Appl. Phys. Lett. 85 (15), 3307–3309.

Wilk, S.J., Petrossian, L., Goryll, M., Thornton, T.J., Goodnick, S.M., Tang, J., Eisenberg, R.S., 2005a. IEEE Sensors. Irvine, CA.

Wilk, S.J., Petrossian, L., Goryll, M., Thornton, T.J., Goodnick, S.M., Tang, J., Eisenberg, R.S., Saraniti, M., Wong, D., Schmidt, J.J., Montemagno, C.D., 2005b. J. Surf. Sci. Nanotechnol. 3, 184–189.

Wonderlin, W.F., Finkel, A., French, R.J., 1990. Biophys. J. 58 (2), 289–297.